Influence of succinic acid species on structural, spectroscopic,optical, Z-scan, frequency doubling, photoconductivity and antibacterial properties of glycine single crystals

N. S. Priya[a], S. A. Chudar Azhagan[b,*]
[a]*Department of Physics, Nehru Institute of Engineering and Technology, Coimbatore, India*
[b]*Department of Physics, Government College of Technology, Coimbatore, India*

With succinic acid as an additive, glycine single crystals were grown by conventional solvent slow evaporation route. Effect of succinic acid on the growth, optical and dielectric properties of glycine polymorphs has been investigated. The occurrence of functional groups has been identified by vibrational FTIR spectrophotometer. The low value of dielectric constant and dielectric loss at higher frequency range attested the grown crystal for frequency doubling applications. The laser damage threshold energy of the grown crystal was calculated. Third order nonlinear susceptibility$\chi^{(3)}$ (esu) of succinic acid added glycine crystals were evaluated from Z-scan experiment.

(Received August 14, 2022; Accepted January 12, 2023)

Keywords: γ-glycine, Succinic acid, Dielectric material, Photonic applications

1. Introduction

The search for new sophisticated NLO materials is a fundamental part of current research to extend the science and communication technology. The ferroelectric materials have extensive variety of industrial applications in optoelectronics field such as capacitors, military services, actuators, telecommunications, non-volatile memory devices, automatic access control systems, high-performance gate insulators and medical equipment's etc [1-2]. Ferroelectric materials become favored materials in a broad range of electronic and mechatronic devices owing to their well-defined dielectric, piezoelectric and pyroelectric properties. Ferroelectric materials with Nonlinear Optical (NLO) property have been a great deal of interest in recent years due to their potential applications in the domain of optoelectronics and photonic technologies. Ferroelectric succinic acid possesses good pyroelectric properties. Succinic acid is a naturally exist organic material that belongs to dicarboxylic acid created as an intermediate of the tricarboxylic acid cycle. It has been generally used in biological and industrial applications and also it has been used as a matrix in infrared (IR) MALDI analytical methods [3-4]. Currently, succinic acid crystals widely used for fabrication of high electron mobility transistor (HEMT). Combination of succinic acid with organic material improved their ferroelectric property [5]. Among the polymorphic crystals, Amino acid glycine is the simplest one which exhibits three different polymorphic forms in ambient conditions viz. α-glycine, β-glycine and γ-glycine. Organic and inorganic complexes of glycine have recently fascinated attraction to scientific community owing to their ferroelectric, dielectric and nonlinear optical properties. The strong piezo-electric and nonlinear optical effect exhibited byγ-glycinecrystals [6-8]. The nonlineara nd dielectric response of glycinepolymorphs is an important parameter for device fabrication applications. For manufacturing nonlinear optical devices, the material ought to have low dielectric constant and low dielectric loss in the higher frequency region. In addition to this decrease R_c delay in microelectronics industry. Now a day's various researchers reported some significant properties of γ-glycine single crystals [9-12]. Thus, in the present investigation, γ-glycine single crystals have been harvested from the succinic acid additive environment.

*Corresponding author: anbuchudarazhagan@gmail.com
https://doi.org/10.15251/DJNB.2023.181.55

2. Glycine crystallization experimental procedure

The crystallization experiment was performed by adding five different molar concentrations of succinic acid additive namely 0.2, 0.4, 0.6, 0.8 and 1 M in saturated glycine solutions to induce alpha and gamma glycine nucleations preferably. The prepared solutions were stirred constantly for 6h using magnetic stirrer at ambient temperature and the solvent used in this experiment was double distilled water. The homogeneous glycine saturated solutions were filtered with Grade no.1Whatman sieve sheets. Finally the filtered solution was watchfully collected in a crystallizing dish and neatly covered with pin pierced polythene sheet and placed in a dust free compartment for controlled slow evaporation. The nucleation started within the interval of 15-30 days, microscopic single crystals were nucleated from the supersaturated glycine solutions. The succinic acid added grown glycine single crystals with respect to various molar concentrations are shown in Fig. 1 (a-e). The nucleation time span for the grown succinic acid added glycine crystals are presented in Table 1 and it confirms that lower molar concentration of succinic acid nucleates faster than higher molar concentration of succinic acid.

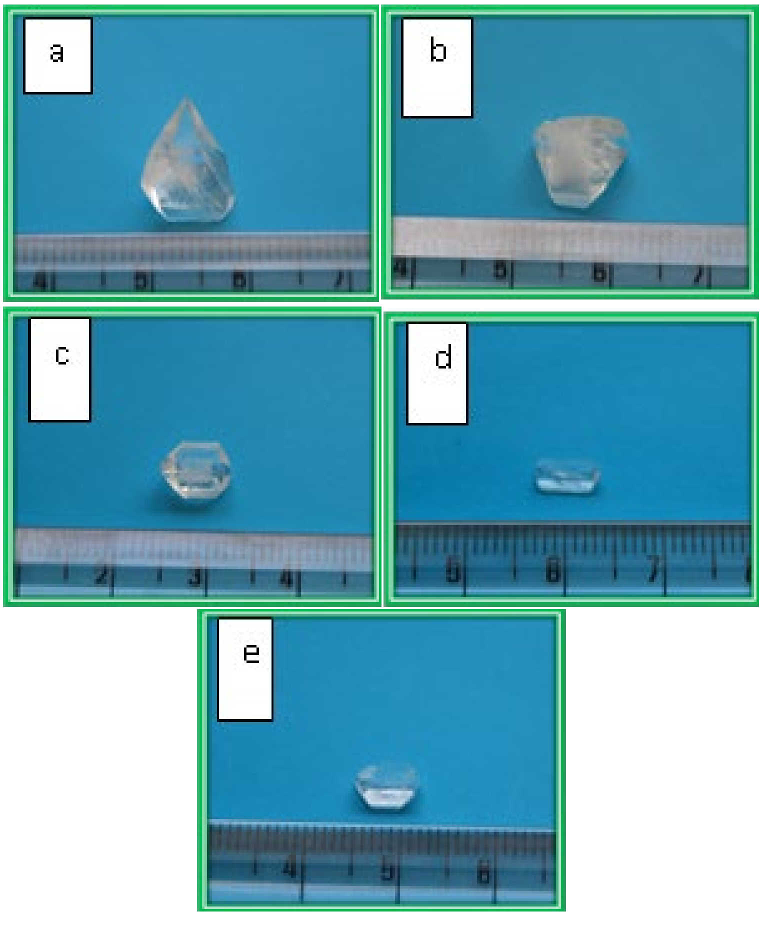

Fig.1. (a-e) Photograph of succinic acid added glycine crystals (0.2M,0.4M,0.6M,0.8M,1 M).

Table 1. Nucleation time span.

Table 1. Nucleation time span

Succinic acid concentration (M)	Sample code	Nucleation in days
0.2	SA1	15
0.4	SA2	17
0.6	SA3	21
0.8	SA4	25
1	SA5	30

3. Results and discussion

3.1.Powder X-ray diffraction analysis

Figure 2 shows the powder XRD diffractogram of grown single crystals and it was recorded by using Bruker AXS D8 Advance X-ray diffractometer with CuKα (λ=1.54 Å) radiation. The scanning rate is 1^0 per min over a range of 10^0–50^0. The crystal structure of the grown crystals were confirmed by prominent diffraction peaks obtained from the diffraction pattern and the result reveals 0.2 M concentration of succinic acid added glycine crystals crystallizes in the monoclinic lattice with centrosymmetric space group P21/n. Also, 0.4-1 M concentration of succinic acid added glycine crystals crystallizes in the hexagonal lattice with non-centrosymmetric space group P_{31}.The reported lattice parameter values are in excellent concurrence with the observed data and the obtained values [13] are tabulated in Table 2.

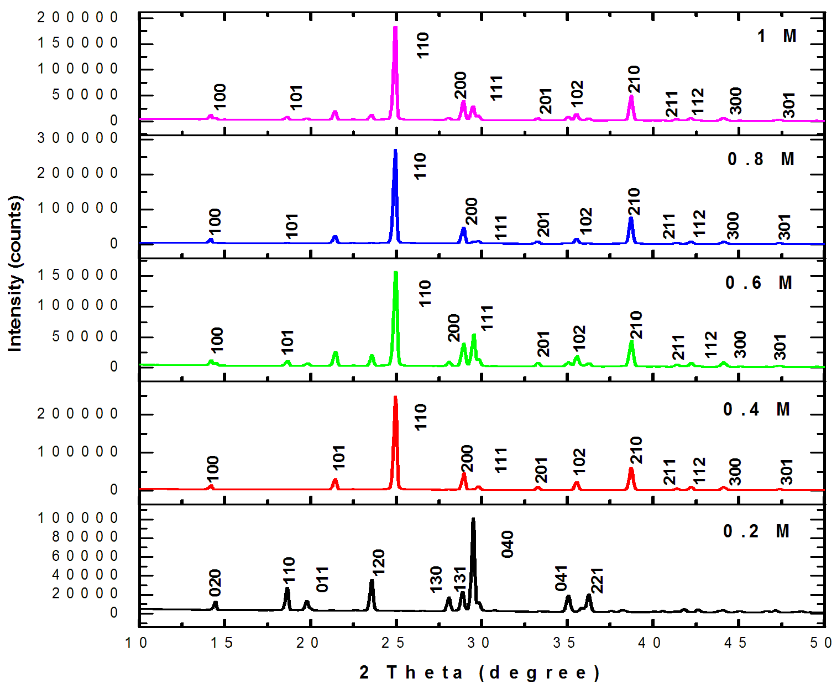

Fig.2. PXRD diffractogram of succinic acid added glycine crystals.

Table 2. SXRD cell parameters of the succinic acid added glycine crystals.

Succinic acid concentration (M)	Polymorphs	Space group	a[Å]	b[Å]	c[Å]	Crystal System
0.2	α	$P2_1/n$	5.51	11.21	5.12	Monoclinic
0.4	γ	$P3_1$	7.19	7.19	5.88	Hexagonal
0.6	γ	$P3_1$	7.01	7.01	5.74	Hexagonal
0.8	γ	$P3_1$	7.13	7.13	5.53	Hexagonal
1	γ	$P3_1$	7.12	7.12	5.86	Hexagonal

3.2.Assignment of vibrational FTIR functional groups

The functional groups present in the compound can be identified by Fourier transforms Infrared (FTIR) vibrational spectrophotometer experiment.The prepared powdered samplesJASCO FTIR spectrum was recorded in the frequency range between 400 and 4000 $cm^{-1}$and it is presented in Fig.3.In the FTIR spectrum of 0.2 M succinic acid added α -glycine single crystal, the presence of sharp peaks at 503, 606 and 691 cm^{-1} are due to the carboxylic group. The presence of peak at 1503 cm^{-1} is corresponds to the ammonium (NH^{3+}) group. Asymmetric mode of C–C–N vibration shows a peak at 1030 cm^{-1} and the presence of peak at 1321 cm^{-1} corresponds to twisting mode of CH_2. The NH^{3+} rocking shows an absorption peak at 1115 cm^{-1} and strong asymmetric CO_2 stretching vibration occurs at 1600 cm^{-1}. The combination bond occurs at 2122 cm^{-1}. The absorption peaks observed at 2607 and 3169 cm^{-1} are due to (NH^{3+}) stretching vibrations of hydrogen bonds. For the remaining crystals such as, 0.4-1 M succinic acid added γ-glycine, the occurrence of peaks at 503-507, 606-608 and 683-695 cm^{-1} are corresponds to the carboxylic groupwhereas the peaks observed at 1479-1495 cm^{-1} corresponds to the ammonium group (NH^{3+}).The existence of IR peaks at 1038-1045 and 889-891cm^{-1} are respectively attributed to C–C–N asymmetric and C–C–N symmetric stretching vibrations. The existence of CH_2 rocking and CH_2 twisting mode at 1321-1334cm^{-1}. The presence of absorption peaks at 1126-1129 cm^{-1} corresponds to NH^{3+} rocking and the existence of band near 2157-2170 cm^{-1} corresponds to combination bond. The absorption peaks exist around 2608-2609 and 3103-3117 cm^{-1} corresponds to (NH^{3+}) stretching vibrations of hydrogen bonds. The assignments of vibrational FTIR functional groups are presented in Table 3. The functional group assignment indicated against grown α and γ-glycine polymorphs are suited with the previous reported research articles [14].

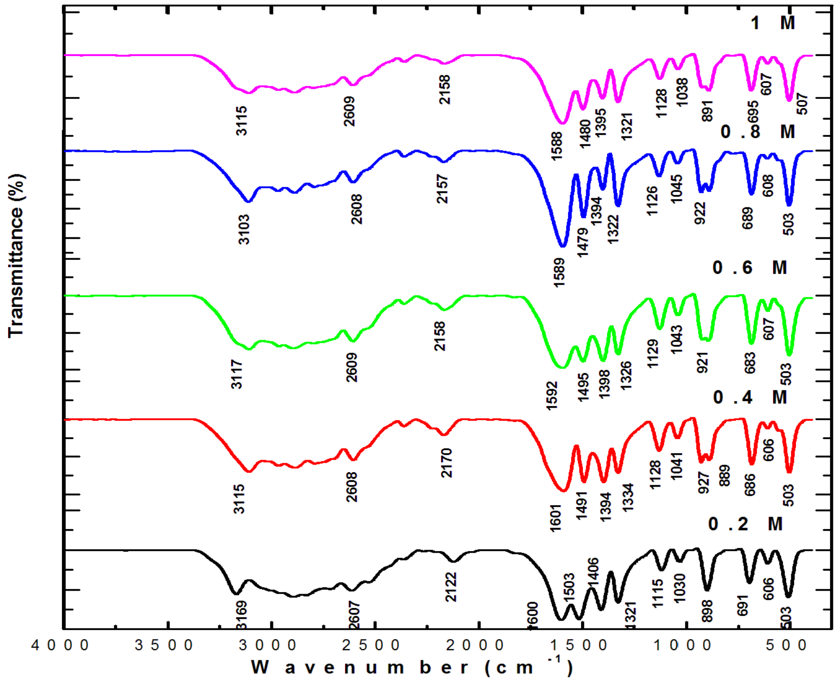

Fig.3. FTIR graph of succinic acid added glycine crystals.

Table 3. FTIR assignment of succinic acid added glycine crystals.

Succinic acid concentration					**Mode of vibrations**
Wave number [cm^{-1}]					
0.2M	**0.4M**	**0.6M**	**0.8M**	**1M**	
503	503	503	503	507	COO^- rocking
606	606	607	608	607	COO^- wagging
691	686	683	689	695	COO^- bending
898	889	887	890	891	CCN symmetric stretching vibration
-	927	921	922	921	CH_2 rocking
1030	1041	1043	1045	1038	CCN asymmetric stretching vibration
1115	1128	1129	1126	1128	NH_3^+ rocking
1321	1334	1326	1322	1321	CH_2 twisting
1406	1394	1398	1394	1395	COO^- symmetric stretching
1503	1491	1495	1479	1495	NH_3^+
1600	1601	1592	1589	1588	Strong asymmetric CO_2 stretching
2122	2170	2158	2157	2158	Combinational bond
2607	2608	2609	2608	2609	NH_3^+ stretching vibration
3169	3115	3117	3103	3115	NH_3^+ stretching vibration

3.3.UV–VIS transmittance studies

The Ultraviolet visible optical transmittance spectrum is a noteworthy feature for nonlinear optical applications, as it gives the information about optical transparency window and lower cut off wavelength of the material. In UV–Visible analysis, three types of electronic transition involved in it such as transition between p, s and n electrons, transition between charge-transfer electrons, transition between d and f electrons. HITACHI, UV double beam spectrophotometer recorded the UV–VIS transmittance spectrum of the powdered glycine samples and is shown in Fig.4. It revealed that the grown succinic acid added glycine crystals attained high optical transmittance range 82-92% in the UV visible region with lower cut-off wavelength between 196 and 236 nm. From the UV spectrum results, occurrence of high optical transmittance in the entire visible region signifies the absence of structural grain boundaries existing in the grown crystals. Owing to this, grown crystals are very useful for optoelectronics and nonlinear optical applications [15-16].

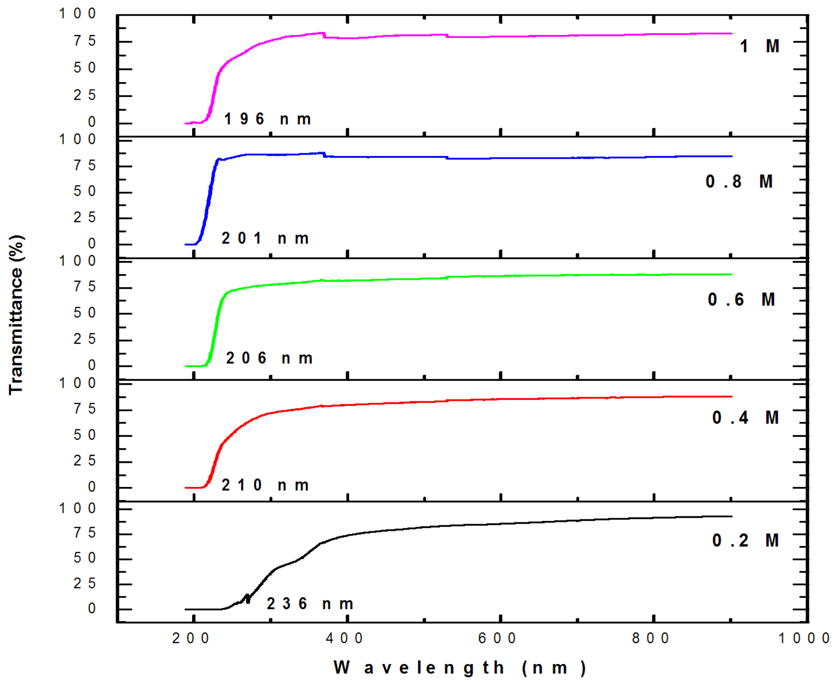

Fig.4. UV-Vis Spectrum of succinic acid added glycine crystals.

3.4. Third order Z-scan nonlinearexamination

To determine both nonlinear index of refraction n_2 and nonlinear absorption coefficient β the Z-scan method is employed. The real [Re$\chi^{(3)}$] and imaginary [Im$\chi^{(3)}$] partof the third-order susceptibility is proportional to nonlinear index of refraction $n_2$and nonlinear absorption coefficient β.The third order nonlinear Z-scan experiment was performed using a diode pumped continuous Wave100 mW, 532 nm diode laser which was focused by a 103 mm focal length lens.The nonlinear parameters calculated from standard formulae [17] and are tabulated in Table 4. The third order Z-scan plot measurements such as, closed aperture, open aperture, division curve CA/OA ratio for succinic acid added glycine crystals are neatly illustrated in Fig.5 (a-c).The third order nonlinear optical susceptibility of the grown material can be computed with the help of division curve Closed Aperture/Open Aperture ratio (Fig.5c). The closed aperture Z-scan trace plotted between normalized transmittance and Z (mm) (Fig.5a) indicates that the pre focal normalized transmittance peak followed by a post focal normalized transmittance valley configuration is the fingerprint of negative nonlinearity (i.e refractive index change is negative) which resulted in self-defocusing behavior in the grown succinic acid added glycine crystals. Moreover, the grown crystals can be employed for protection of optical sensors based applications. The information such as nonlinear optical absorption properties and the nonlinear refractive index change could be derived from Z-scan experiment. The Z-scan principle states that nonlinear optical absorption falls in two categories such as saturable absorption or multi photon absorption and reverse saturable absorption or two photon absorption. When the sample transmittance augments with increasing optical intensity is called saturable absorption where as in reverse saturable absorption the sample transmittance decreases when the optical intensity is increased. Materials belong to saturable absorption, maximum transmittance in focus at peak is present where as in reverse saturable absorption, minimum transmittance in the focus at valley is present. From the open aperture Z-scan trace experiment (Fig. 5b), it is confirmed that two photon absorption or reverse saturable absorption occurred in the succinic acid added grown glycine crystal.

Table 4. Measured third order nonlinear parameters of the succinic acid added glycine crystals.

Sample Code	**n_o**	**n_2 (cm^2/W)**	**α**	**β(cm/W)**	**Re$\chi^{(3)}$ (cm^2/W)**	**Im$\chi^{(3)}$ (cm/W)**	**$\chi^{(3)}$ (esu)**
SA1	2.36	2.64E-11	0.3688	1.34E-06	3.73E-09	8.04E-08	8.05E-08
SA2	2.352	8.68E-11	0.2443	2.75E-06	1.22E-09	1.63E-08	1.64E-08
SA3	2.34	6.27E-11	0.0604	1.02E-06	8.71E-09	6.00E-08	6.06E-08
SA4	2.348	8.47E-11	0.2034	1.67E-06	1.19E-09	9.90E-08	9.97E-08
SA5	2.357	4.76E-11	0.237	6.74E-06	6.71E-09	4.02E-08	4.08E-08

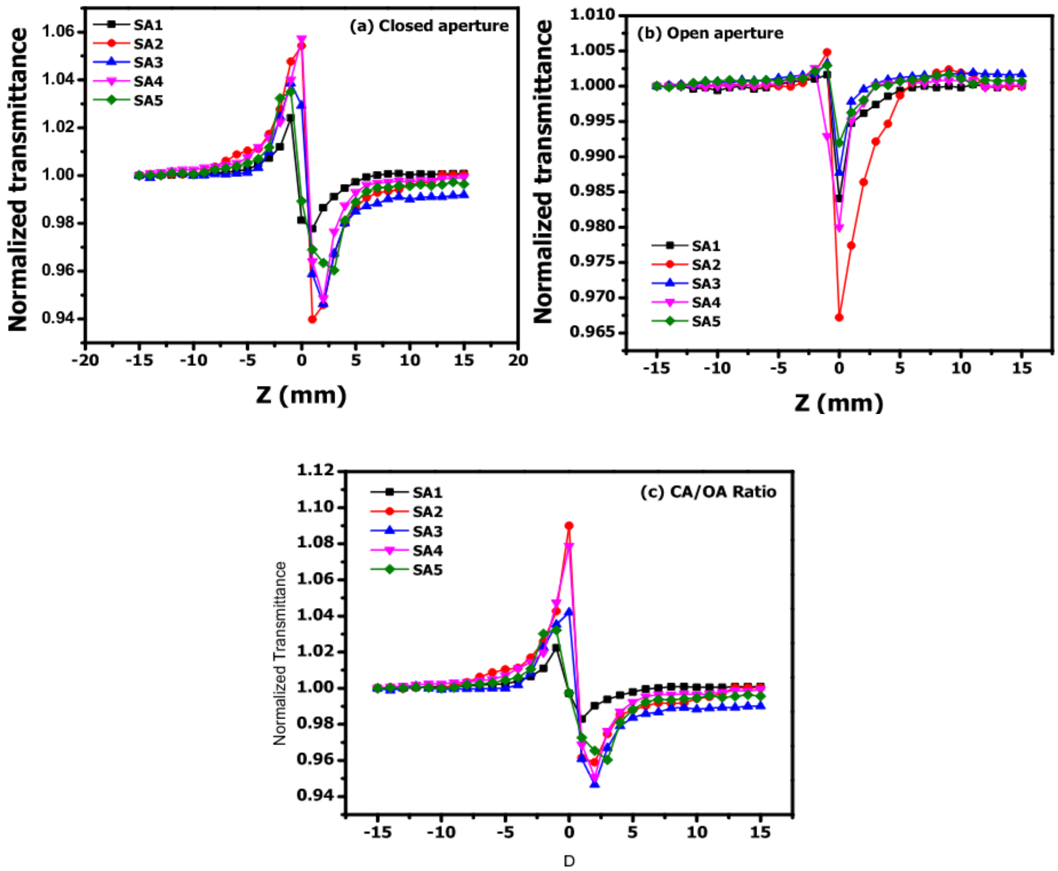

Fig.5. (a) SA+Gly Closed aperture (b) SA+Gly Open aperture (c) SA+Gly ratio of closed to open aperture z-scan plot.

3.5. Dielectric measurement

The Dielectric measurements of the grown crystals give the information about the distribution of the electric field within the crystal, lattice dynamics, transport phenomena and their polarization mechanism. The dielectric constant and dielectric loss of the crystal is reliant on the displacement of polarized charges. Dielectric studies were employed for the grown higher molar concentration (1 M) of succinic acid added glycine crystals at different frequencies and temperatures. Fig. 6 (a-b) shows the variation of dielectric constant with various temperature and various frequencies.The high value of dielectric constant at 40-120°C goes on decreasing with an increase in frequency. At lower frequencies, the higher value of dielectric constant is due to the contribution of electronic, ionic, dipolar and space charge polarizations. If the frequencies augmented, space charge polarization gets decreased; this results in decrease in dielectric constant value. In general, the low value of dielectric constant of crystal is a vital requirement, which creates it a potential candidate for microelectronic, optoelectronic and nonlinear optical industries applications. Also, SHG coefficient is improved owing to the low value of dielectric constant at higher frequencies is in agreement with Miller's rule [18-20]. Fig. 7 (a-b) shows the variation of dielectric loss with various temperature with respect to various frequencies. Dielectric loss values of grown crystal were found to decrease with increasing frequencies. The very low dielectric loss value of grown crystal at high frequency range improves the optical quality of material with minimum defects, which plays an essential role in manufacturing nonlinear optical devices [21].

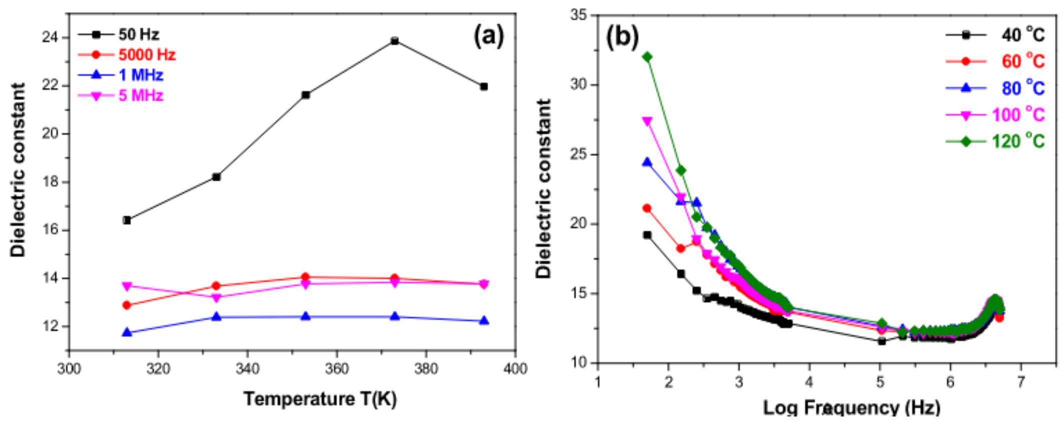

Fig.6. Plot of dielectric constant with respect to (a) frequency and (b) temperature.

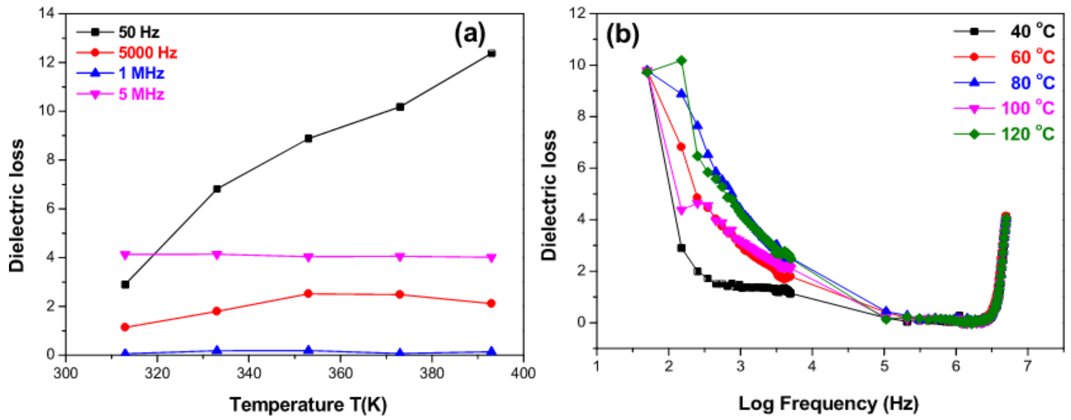

Fig.7. Plot of dielectric loss with respect to (a) frequency and (b) temperature.

3.6. AC conductivity studies

The ac conductivity was calculated using the formula $\sigma_{ac} = \omega\varepsilon_0\varepsilon'\varepsilon''$, where $\varepsilon_0' = 8.854 \times 10^{-12}$ Fm^{-1} is the vacuum permittivity, ε′ is the dielectric constant of the material and ε″ is the dielectric loss of material. The variation of the σ_{ac}conductivity for the sample withdifferent temperature and different frequency was depicted in Fig.8 (a-b). σ_{ac}conductivity increases with increase of temperature and it is due to the transfer of electric charge carriers to the thermally excited donor levels of the conduction band [22]. From the Fig. 8b, it has been observed that σ_{ac} increases with increase of frequency for all the temperatures and hence it can be confirmed that the prepared single crystals are very useful for various microelectronic and optical applications.

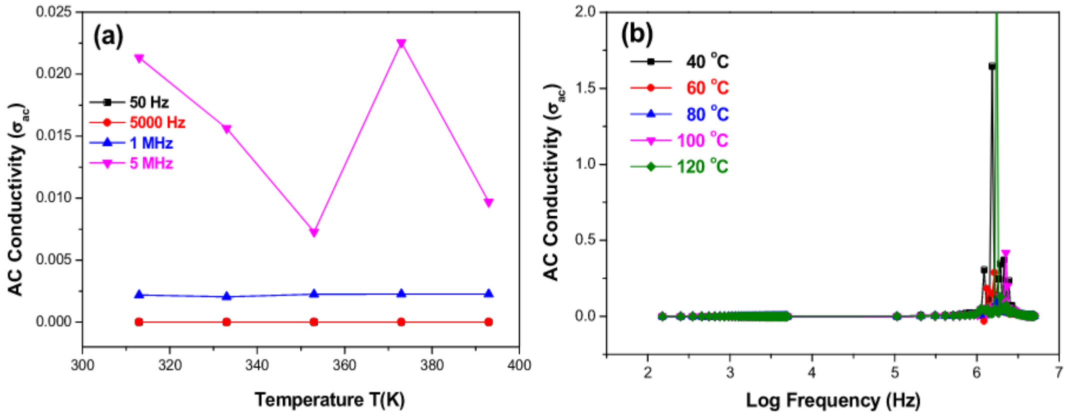

Fig.8. Conductivity with respect to (a) frequency and (b) temperature for the succinic acid added glycine single crystals.

3.7. Impedance analysis

The Cole-Cole plot for succinic acid added glycinesingle crystals is shown in Fig. 9 (a -b). The bulk resistance (R_b) has been calculated from the high-frequency intercept of the semicircle or the low-frequency spike on the real axis (Z′). The ionic conductivity has been evaluated at 3.38×10^{-5} Scm^{-1} [23].The plot of σ_{ac} against 1000/T for the frequencies 50, 5000, 1 MHz and 5 MHz values are found to be linear. The activation energy was calculated by fitting the curve using Arrhenius formula [24]. Figure 9b represents the temperature dependence of ionic conductivity for the crystal is in the range of temperature from 313 to 393 K. It has been found that the ionic conductivity of the sample increases with increasing temperature. By using the linear fit of the Arrhenius plot, the average activation energy has been calculated for the crystal and the values are found to be 0.72 eV.

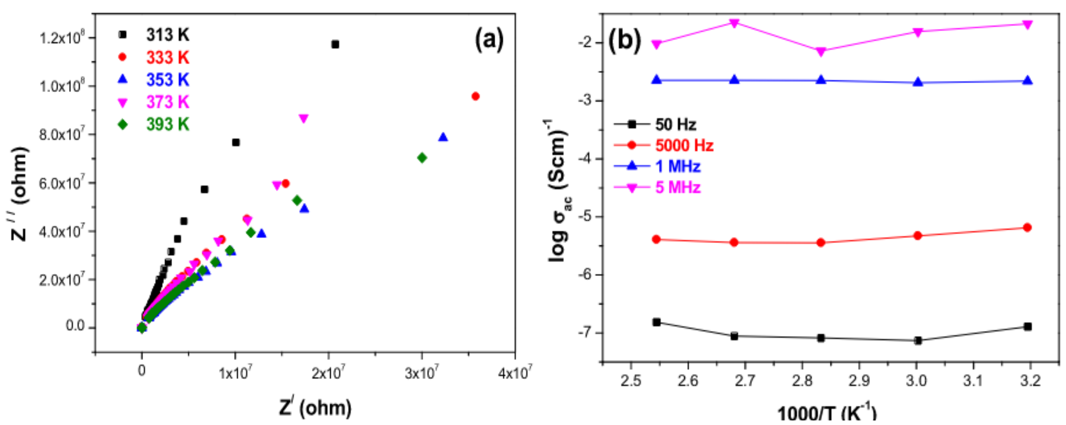

Fig. 9. (a) Cole-Cole plots and (b) temperature dependence of ionic conductivity of the succinic acid added glycine single crystals.

3.8. Photoconductivity studies

The grown 1 M of succinic acid added glycine crystal was connected in series to DC power supply and Keithley Model 6517B Electrometer. The applied input voltage was increased in steps of 1V to record the photocurrent (I_p) and dark current (I_d) produced by the grown γ-glycine crystal is depicted in Fig.10.The result revealed that both dark current and photocurrents are linearly increases with the applied electric field but dark current is superior to the photo current at every applied electric field. From the results, γ-glycine single crystal grown from succinic acid possesses a negative photoconductivity which is due to the drop in the number of charge carriers or decrease in their lifetime on illumination. When light is illuminated on the crystal, recombination of electrons and holes takes place, dipping the number of mobile charge carriers foremost to negative photoconductivity and decreases lifetime of the charge carriers [21].

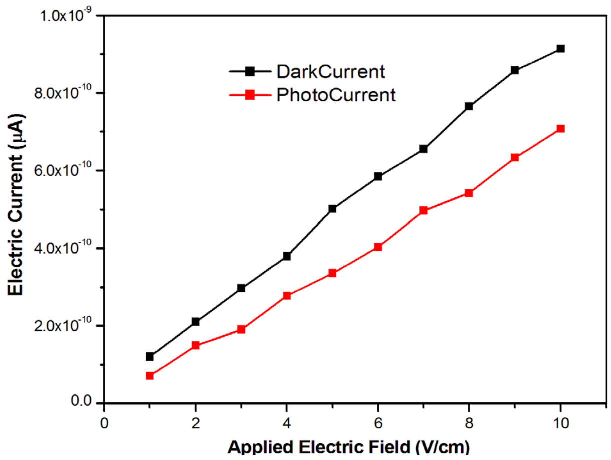

Fig. 10. Photoconductivity response curve of the succinic acid added glycine crystals.

3.9. Powder second harmonic generationanalysis

The effectiveness of a nonlinear optical material can be persistent by second harmonic generation efficiency (SHG) factor which provides the efficiency of transferring energy from an elementary beam to second harmonic beam. In order to find the SHG behavior of the grown crystal Kurtz powder technique is one of the most widely used techniques [25]. The grown glycine crystals were finely grounded and compactly packed in a micro capillary glass tube. A Nd:YAG Q-switched laser of 1064 nm, generating an 8 ns pulse and operating at 1.6 mJ/pulse and at a rate of 10 Hz, is excited at the right angle and distance in order to notice visibly the SHG in the green color region (532 nm), the predictable emitted half wavelength signal. Subsequently, the green light output was photographed in order to support the double-frequency emission. The powdered KDP crystal was used as a reference material for this test. The obtained result shows that SHG conversion efficiency of KDP is 28 mV. The powder SHG efficiency of grown 0.2-1 M of succinic acid added crystals are 0.32 (9 mV), 0.61 (17 mV), 0.89 (25 mV) and 1.04 (29 mV) times that of reference KDP. The SHG efficiency of γ-glycine crystals grown from succinic acid was found to be higher than many other reported non-linear optical γ-glycine crystals[8-13]. Hence, noticed SHG property proves the suitability of grown γ-glycine for NLO device applications.

3.10. Measurement of laser damage threshold (LDT)

The optical damage threshold energy for an optical crystal is measured as energy per area or intensity (power per area) and wavelength. [26]. Optical damage threshold studies have been carried out for grown 1 M of succinic acid added glycine crystal using Q switched Nd: YAG laser of pulse width 10 nano seconds and repetition rate of 10 Hz. The grown crystals were cut and polished into a rectangular slab of thickness 5 mm and then the laser damage threshold energy was measured. The laser beam was focused and the sample was moved step by step into the focus along the optical axis of the crystal. Initially 10 mJ was applied on the surface of the crystal and no damage is seen upto 30s and then the energy is increased to 16 mJ/pulse, a small dot like damage is spotted on the crystal. This energy is noted as threshold energy for that crystal. A significant damage is noticed when the energy is increased to 20 mJ/pulse and the crystal completely breaks.

3.11. Antibacterial activity evaluation

The zone of inhibitions (ZOI) exhibited by the five different molar concentrationsof 0.2 to 1 M insteps of 0.2 M powdered samples of succinic acid added glycine single crystals are depicted in Fig. 11 (a–e). The five microorganisms studied at 1 M concentration of the powdered glycine sample were *Vibrio cholerae* (12 mm ZOI), *Bacillus cereus*(12 mm ZOI), *Pseudomonas aeruginosa*(12 mm ZOI), *Staphylococcusaureus*(11 mm ZOI) and*Escherichia coli* (12 mm ZOI)exhibiting moderate antibacterial activity against these pathogens when compared to other pathogens studied by Murugavel *et al.* (2015) [27] and Vijayalakshmi *et al.* (2018) [28] and.

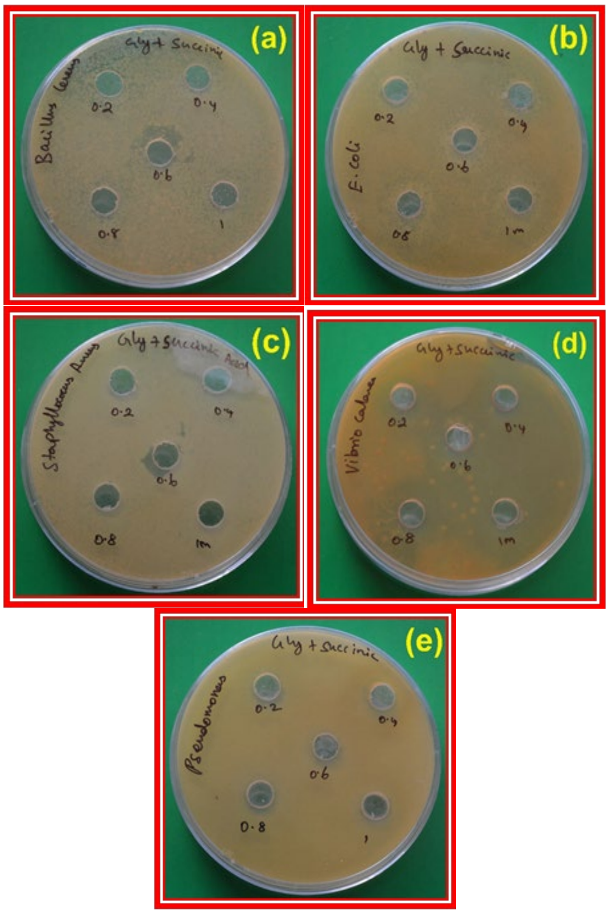

Fig. 11. (a-e) Photographic view showing zone inhibition of five different micro-organisms at concentrations (0.2, 0.4, 0.6, 0.8 and 1 M) against succinic acid added glycine crystals.

In the present work, it is evident that the grown dicarboxylic acid succinic acid added glycine single crystals have shown reasonable dominance towards gram negative bacterial assay microorganism V*ibrio cholerae*, *Pseudomonas aeruginosa* and gram-positive bacterial assay microorganism *Bacillus cereus* except gram positive microorganism *Staphylococcusaureus*(11 mm ZOI)and shown their ZOI impact variation against change of molar concentration of succinic acid. The grown succinic added powdered glycine samples exhibited moderate antimicrobial activity ranging from 11-12 mm inhibition zone diameter for almost all pathogens as tabulated in Table 5. Among the five pathogenic bacteria strains, all the four microorganism shows moderate diameter of inhibition zones (12 mm ZOI) except *Staphylococcusaureus*(11 mm ZOI). From the zone of inhibition table end result (Table 5), it is concluded that higher molar concentration of succinic acid added glycine single crystals gives improved results and good sensitivity when compared to lower molar concentration of succinic acid added single crystals (Renuka 2014) [29]. The enhanced sensitivity towards higher concentration of one molar concentration 1M added succinic acid added glycine single crystals follows the sequence as *Vibrio cholera =Bacillus cereus = Pseudomonas aeruginosa*, = *Escherichia coli > Staphylococcus aureus.*

Table 5. Effective values of inhibition zone for succinic acid added glycine crystals at concentrations (0.2, 0.4, 0.6, 0.8 and 1.0 M) against selected bacteria.

Succinic acid concentration (M)	**Zone of inhibition (mm) (activity index)^{std}**				
	Bacillus cereus	***Staphylococcus***	***E.coli***	***Vibrio cholera***	***Pseudomonas aeruginosa***
0.2	11	11	11	12	11
0.4	11	11	11	12	12
0.6	12	11	11	12	12
0.8	12	11	12	12	12
1	12	11	12	12	12

4. Conclusion

Succinic acid added glycine crystals have been successfully grown using slow evaporation solution growth technique. The cell parameters and crystal structure were determined from PXRD analysis. FTIR spectrum identified the functional groups in grown crystals. High optical transparency along with lower cut off wavelength is the right choiceof material for optoelectronics and device fabrication applications. The low value of dielectric constant and dielectric loss at higher frequencies are the promising criterion for NLO applications. γ-glycine single crystal grown from succinic acid possesses a negative photoconducting nature. Third order nonlinear optical Z-scan investigation reveals that closed and open aperture Z-scan trace confirms the self defocusing effect and two photon absorption in the grown material. Optical laser damage threshold studies confirmed that crystal breaks when the threshold energy reached 20mJ per pulse. Better SHG efficiency confirmed the non-linear optical nature of grown crystal. Thus, succinic acid added glycine crystal is a potential material for piezoelectric, optoelectronics devices, non-volatile memory device applications due to its optical and dielectric behavior. The obtained results proved that the grown succinic acid doped glycine single crystals are exhibiting better antimicrobial activity against both gram-negative bacteria and gram-positive bacteria.

Acknowledgements

The author acknowledges the Sophisticated Analytical instrumental Facility centre (STIC), Cochinand G.Vinitha,VIT University for providing the characterization facilities.

References

[1] S.Krishnan, C.Justin Raj, R.Robert, A.Ramanand, S.Jerome Das, Cryst. Res. Technol. 42 (11), 1087 (2007); https://doi.org/10.1002/crat.200710981
[2] Y. K.Hong, W. H.Hong, H. N. Chang, Biotechnol. Lett. 22, 871 (2000); https://doi.org/10.1023/A:1005627816323
[3] J. F.Remenar, S.L.Morissette, M.L.Peterson, B.Moulton, J.M.Macphee, R.Guzma, J. Am.

Chem. Soc. 125 (28), 8456 (2003); https://doi.org/10.1021/ja035776p
[4] M. A.Carnahan, C.Middleton, J.Kim, T.Kim, M. W. Grinstaff, J. Am. Chem. Soc. 124 (19), 5291 (2002); https://doi.org/10.1021/ja025576y
[5] J.Hagberg, J Chromatogr A. 988 (1), 127 (2003); https://doi.org/10.1016/S0021-9673(02)02022-8
[6] Jin Hee Lee, Jae Yeob Shim, Hyung Sup Yoon, Hae Cheon Kim, J. Korean Phys. Soc. 42, s662 (2003).
[7] C.Sekar, R.Parimaladevi, Spectrochim. Acta: A. 74 (5), 1160 (2009); https://doi.org/10.1016/j.saa.2009.09.026
[8] K. Ambujam, S. Selvakumar, D. P.Anand, G.Mohamed, P.Sagayaraj, Cryst.Res.Technol.41 (7), 671 (2006); https://doi.org/10.1002/crat.200510647
[9] M.N.Bhat, S. M. Dharmaprakash, J. Cryst. Growth. 236 (1-3), 376 (2002); https://doi.org/10.1016/S0022-0248(01)02094-2
[10] R. Parimaladevi, C.Sekar, Spectrochim. Acta: A. 76 (5), 490 (2010); https://doi.org/10.1016/j.saa.2010.04.008
[11] G.R.Dillip, P.Raghavaiah, K.Mallikarjuna, C.MadhukarReddy, G.Bhagavannarayana, V. Ramesh Kumar, B. Deva Prasad Raju, Spectrochim. Acta: A. 79 (5) 1123 (2011); https://doi.org/10.1016/j.saa.2011.04.031
[12] Mohd Anis, S.P.Ramteke, M.D. Shirsat, G.G. Muley, M.I.Baig, Optical Materials. 72, 590 (2017); https://doi.org/10.1016/j.optmat.2017.07.007
[13] R.Ashok Kumar, R.Ezhil Vizhi, N.Sivakumar, N.Vijayan, D.Rajan Babu, Optik. 123 (5), 409 (2012); https://doi.org/10.1016/j.ijleo.2011.04.019
[14] S.Anbuchudar Azhagan, S.Ganesan, Optik. 123 (11), 993 (2012); https://doi.org/10.1016/j.ijleo.2011.06.063
[15] S.Anbuchudar Azhagan, S. Ganesan, Optik. 124 (20), 4452 (2013); https://doi.org/10.1016/j.ijleo.2013.02.019
[16] S.P Ramteke, Mohd Anis, M.I.Baig, V.G.Pahurkar, G.G. Muley, Optik. 137, 31 (2017); https://doi.org/10.1016/j.ijleo.2017.02.096
[17] P.Sangeetha, P.Jayaprakash, M.Nageshwari, C.Rathika Thaya Kumari, S.Sudha, M.Prakash, G.Vinitha, M.Lydia Caroline, Physica B: Condensed Matter 525 164 (2017); https://doi.org/10.1016/j.physb.2017.08.037
[18]. M.I.Baig, Mohd Anis, G.G. Muley, Optik, 131, 165 (2017); https://doi.org/10.1016/j.ijleo.2016.11.085
[19] M.Anis, G.G. Muley, Opt. Laser Technol. 90, 190 (2017); https://doi.org/10.1016/j.optlastec.2016.11.020
[20] C.Justin Raj, S.Dinakaran, S.Krishnan, B.Milton Boaz, R.Robert, S.Jerome Das, Opt. Commun. 281 (8), 2285 (2008); https://doi.org/10.1016/j.optcom.2007.12.019
[21] V.Joseph, S.Gunasekaran, V.Santhanam, Bull. Mater. Sci. 26, 383 (2003); https://doi.org/10.1007/BF02711180
[22] S. Abed, H. Bougharraf, K. Bouchouit, Z.Sofiani, B.Derkowska-Zielinska, MS Aida, B Sahraoui,Superlattices and Microstructures. 85, 370 (2015); https://doi.org/10.1016/j.spmi.2015.06.008
[23] BA Boukamp, Solid State Ionics, 20, 31 (1968); https://doi.org/10.1016/0167-2738(86)90031-7
[24] K. K. Harjinder Singh, Bamzai, Journal of Materials Science: Materials in Electronics. 30 (4), (2019).
[25] S.K Kurtz, T.T. Perry, J. Appl. Phys. 39, 3798 (1968); https://doi.org/10.1063/1.1656857
[26] C.Ignatius, S.Rajathi, K.Kirubavathi, K.Selvaraju, J. Nonlinear Opt. Phys. Mater. 25 (2), 1650017 (2016); https://doi.org/10.1142/S021886351650017X
[27] S. Murugavel, N. Manikandan, D.Lakshmanan, Kanagaraj Naveen, Paramasivan Thirumalaiperumal, J. Chil. Chem.Soc. 60 (2), 3015 (2015).

[28] V.Vijayalakshmi, P. Dhanasekaran, N.M. Ganesan, Molecular Crystals and Liquid Crystals, 664 (1), 241 (2018); https://doi.org/10.1080/15421406.2018.1473994
[29] V. Renuga, International Journal of Scientific Research, 3 2277 (2014).